Aerosol transmission and air quality in a generic conference room – comparison of aerosol- and tracer-gas-based methods

Michael Mommert[1*] and *Andreas* Westhoff[1]

[1] German Aerospace Center (DLR), Institute of Aerodynamics and Flow Technology, Department Ground Vehicles, Bunsenstr. 10, 37073 Göttingen, Germany

Abstract. Assessing air quality indicators, including the age of air, by means of tracer-gas measurements is a prevalent technique used to evaluate the effectiveness of indoor ventilation systems. The COVID-19 pandemic has recently drawn attention to the transmission of pathogens via indoor air flows. Measurement techniques for the investigation and characterization of ventilation effects have moved from global to local measurements, using local aerosol sources and particle sensors to determine the aerosol dispersion of specific source-receptor combinations. The study at hand introduces a new test environment that can be used to carry out such investigations. It is a n modular conference room equipped with 20 thermal manikins that simulate the obstruction and heat release of a human body. The study further aims to determine the capacity to estimate air age using investigations that involve distributed or local tracer injections.

1 Motivation

The COVID-19 pandemic has shifted the priority of indoor ventilation solutions from energy efficiency and thermal comfort to reducing the concentration and spread of pathogens. In particular, meeting places such as conference rooms or classrooms have received a lot of attention in research to understand and mitigate the spread of pathogens [1-3]. However, most of these are numerical studies. With the objective to provide a real environment, we build a generic conference room to test different ventilation concepts or for the validation of numerical simulations. It is presented in section 2.

With this change of focus due to the pandemic, the applied air quality measurement techniques also shifted from global methods, such as age of air (AoA) determinations with tracer gas, to local methods, such as studying the distribution of tracers emitted by individual sources. In our test environment we are able to accommodate the equipment needed for both of these approaches. The respective experimental setups are described in section 3.

Since all included measurement techniques provide data to investigate the concentration decay at the different sensor locations after source deactivation, we also wanted to investigate the following question: Can studies with local sources also be used to reliably estimate the AoA with the step-down method? According to theory, sufficient mixing is required for this purpose [4]. Therefore, we use AoA values determined by injecting CO2 into the supply air, which guarantees this mixing, as a reference for the investigations in sections 4 and 5.

2 Generic conference room

2.1 General information

To investigate the above aspects, a generic room was set up. The side lengths are 5.5 m and 4.8 m and the height is 2.6 m. Hence, the floor area is 26.4 m² and the volume is 68.6 m³. The walls were modularly designed using timber construction segments to allow future changes to the floor plan. The side walls and the ceiling are equipped with an 80 mm thick internal thermal insulation made of extruded polystyrene hard foam (0.036 W/(m·K)).

In order to reflect the scenario of a conference or class room, the floor plan was designed with 10 desks (1×0.6) m² with two seats each.

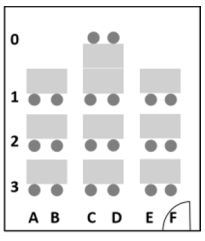

Fig. 1. Floor plan of the generic conference room.

The floor plan of Fig. 1 reveals the coordinates to label the seating positions. For the experiments presented in this paper, each position was occupied by a thermal manikin [5] emitting 70 W of heat.

* Corresponding author: michael.mommert@dlr.de

2.2 Ventilation scenarios

The air quality and aerosol transmission studies include the testing of several ventilation concepts listed in the following table:

Table 1. Investigated ventilation concepts are marked with their abbreviation inside the test matrix.

Flow rate → **↓ Description**	**900 m³/h**	**450 m³/h**
Wall-based ventilation unit	W+	W-
Parapet ventilation unit		P-
Ceiling-based ventilation unit	C+	C-
Low-momentum ventilation concept	L+	L-

The scenarios represent different ventilation units placed at different positions in the room. All units were equipped with a heat recovery system and were supplied with the corresponding air flow rate, which was conditioned to a temperature between 10 °C and 11 °C. All tests were performed with 100 % fresh air supply, i.e. without air recirculation.

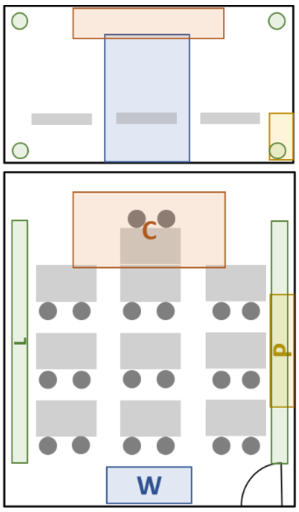

Fig. 2. Floor plan (bottom) an elevation (top) sketches of the ventilation unit placement for the wall (W), parapet (P) and ceiling (C) units as well as the low-momentum-ventilation (L).

The positions of the units are depicted in Fig. 2. The wall and ceiling units were permanently installed in the room. Both the parapet unit and the extended ducts used for the low-momentum concept were only installed for the respective tests.

The single units had separate inlet and outlet fans. These have been adjusted so that they deliver the desired flow rate and provide a neutral pressure in the room in relation to the surroundings. Details of the ventilation concepts are presented in the following subsections.

2.2.1 Wall-based ventilation unit

Fig. 3 shows a photo of the wall-mounted ventilation unit. It collects the stale air in an outlet next to its feet, which points downwards. Fresh air is supplied through two inlets at the top of the unit, which point upwards into the room.

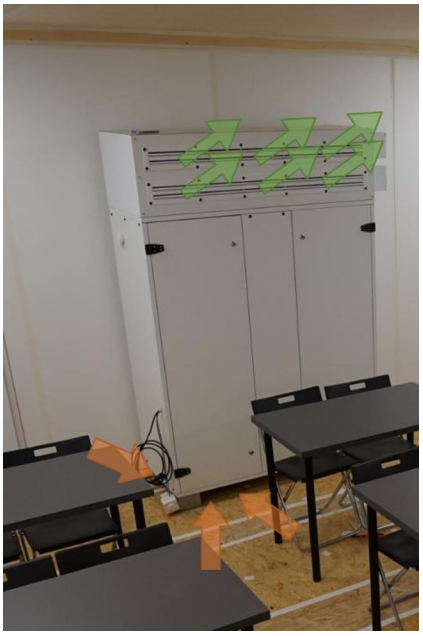

Fig. 3. Photo of the installed wall-based unit with arrows highlighting the induced air flow.

2.2.2 Parapet ventilation unit

The unit for parapet mounting, is depicted in Fig. 4. It distributes fresh air along the floor through the inlets at the bottom. The stale air is collected at the higher located outlets. Both types of openings face the room.

Fig. 4. Photo of the installed parapet unit with arrows highlighting the induced air flow.

2.2.3 Ceiling-based ventilation unit

The ceiling unit is shown in Fig. 5. Its inlet for the distribution of fresh air is directed downwards, but the air flow is directed into the room by means of a lamellar insert using the Coandă effect. The used air is collected in a downward-facing outlet located closer to the wall.

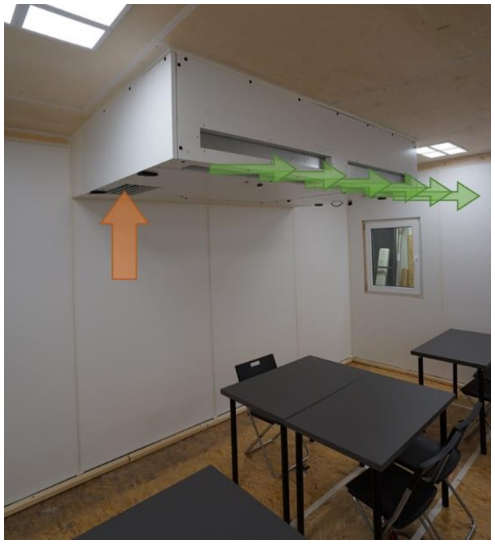

Fig. 5. Photo of the installed ceiling-based unit with arrows highlighting the induced air flow.

2.2.4 Low-momentum ventilation

For the low-momentum ventilation system, the ceiling mounted unit has been extended. The fresh air is fed through a ducting to the lower longitudinal edges of the room. There, the fresh air is distributed through perforated pipes (length 4 m, Ø 150 mm), which were covered with hoses. These hoses had sections of a quarter of their circumference made of permeable textile (approx. 1800 m³/(h·m²) at 200 Pa). These sections acted as low-momentum inlets and provided the resistance to distribute the flow along the length of the perforated tube.

The stale air is collected at the respective upper edges of the room and transported to the ceiling unit via ducting. Because of the prototype nature of this arrangement, the ducting was installed within the room. Fig. 6 shows a photo of the installation of the low-momentum ventilation.

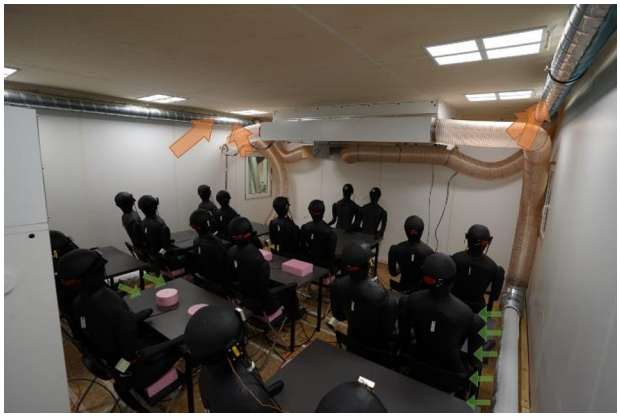

Fig. 6. Photo of the low-momentum extension applied to the ceiling-based unit with arrows highlighting the induced air flow.

3 Experimental Setup

3.1 CO_2 tracer gas system

The concentration of CO_2 is an essential characteristic of the perceived air quality in a room, as symptoms caused by elevated concentrations can be observed already from 1000 ppm [6], which is regularly exceeded [7].

Therefore, an exhalation simulation was developed to investigate the performance of ventilation concepts with regard to this aspect. For this purpose, compressed air and CO_2 are combined in a gas mixing unit equipped with a buffer vessel with a capacity of 100 l. From there, the CO_2-enriched air is fed to the individual manikins via a tube system with capillary sections at each manikin for a uniform distribution. The exhalation jet is simulated by means of 3D-printed nose extensions of the manikins, as shown in Fig. 7. For the exhalation studies, each manikin exhaled a mixture of air and 4.5 % CO_2 at a constant flow rate of 7.5 l/min.

In addition, the system can also be used to perform tracer gas measurements using the more established method of centrally injecting the gas or, in this instance, the enriched gas mixture. For these investigations, the gas was injected into the supply connection of the ventilation units. Since the inlet fans follow the injection site downstream, sufficient mixing can be assumed for step-down AoA measurements.

In both cases, information about the distribution of the tracer gas was acquired with Sensirion SCD30 CO_2 sensors. They were implemented in pairs in the outlet compartments of the respective ventilation units. Further, one sensor was assigned to each desk. The sensors were installed on the inner temples of a manikin for measuring the CO_2 concentration in the vicinity of the face - but not directly in the exhaling jet. An example of this sensor placement is shown in Fig. 7.

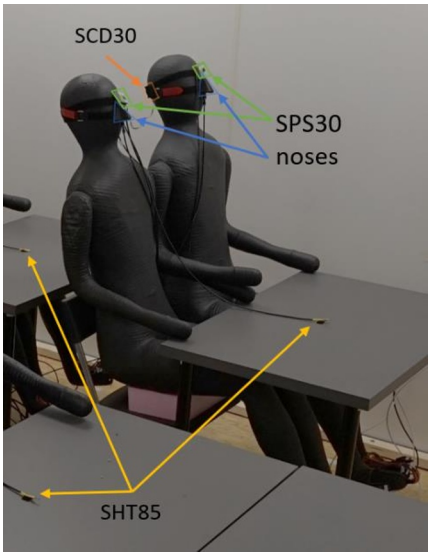

Fig. 7. Position of the temperature (SHT85), CO_2 (SCD30) and particle (SPS30) sensors in relation to the noses of the exhalation simulation.

3.2 Aerosol distribution system

To measure the aerosol distribution in the room, a particle generator using artificial saliva and producing particles with a size between 0.3 and 2.5 µm [8] was installed in the room. The generator was connected to a face mask that produced a combined nasal and oral jet, simulating a local aerosol source. For each ventilation scenario, the two source positions of D2 (pos. I) and A2 (pos. II) were investigated. Its use at position I is shown in Fig. 8.

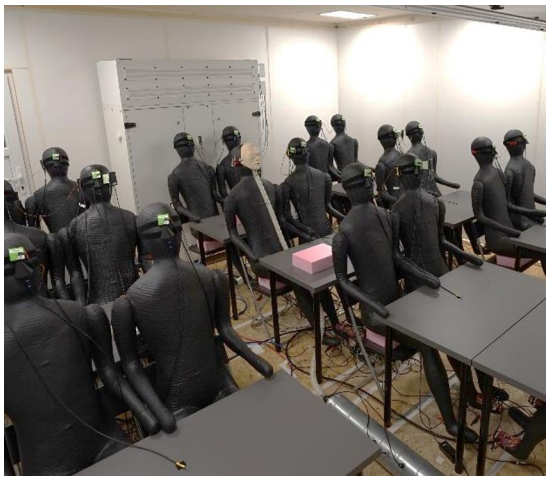

Fig. 8. Installation of the aerosol source on position I at seat D2.

Similar to the CO_2 measurements, a sensor array was used to determine the spatial aerosol distribution. This setup consists of 2 sensors in the outlet compartments of the respective ventilation units and sensors for each seat except for the source position.

For this purpose, Sensirion SPS30 sensors were installed on the foreheads of the manikins (see Fig. 7). This way, they are positioned within the breathing zone of the occupants without being influenced by the exhaling jet, as the exhalation simulation was also active for the aerosol-based tests. There, the exhalation volume flow is 7,5 l\min of air for each manikin except for the particle source.

3.3 Temperature measurements

For the measurement of temperatures, Sensirion SHT85 sensors were used. Two sensors monitoring the temperature of the environmental air supplied into the ventilation units were positioned a short distance upstream of the units with the respective channel. To measure the temperature near of the thermal manikins further sensors were installed in the center on top of each desk.

All sensors, aerosol, CO_2 and temperature, were connected to data acquisition systems as described by Niehaus et al. [9].

4 Age of Air evaluation

Since all of the experimental techniques presented in section 3 provide the time decay of the respective concentrations, it is possible to determine the corresponding AoA values based on the step-down method.

However, both CO_2 and the salvia particles have a background concentration below which the concentrations do not fall. To determine the AoA values close to the integral approach, based on the ASHRAE standard 129 [10], the following algorithm was applied to both types of time series.

For the description of the algorithm, the data set of one of the exhaust sensors in scenario W+, measured for the exhalation simulation, is used as an example. It is shown in Fig. 9.

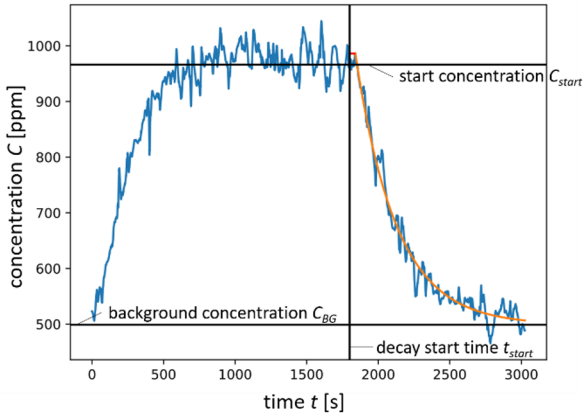

Fig. 9. CO2 time series of an outlet sensor for scenario W+ measured for the exhalation scenario.

In this plot, the start time of the decay t_{start} which corresponds to the time the CO_2 injection was stopped, is marked by a vertical line. In addition, the plot shows, that the exponential decay at the sensor position starts with a delay Δt, which is part of the AoA. To account for this delay, a series of curve fits of the function $f(t, [\tau, C_{BG}]) = C(t_{start} + \Delta t) \cdot \mathrm{e}^{-(t-t_{start}-\Delta t)/\tau} + C_{BG}$ to the raw data are performed for increasing Δt. From this series of fits, the one with the smallest least squares deviation to the raw data is selected for further evaluation, as it represents the fit that best captures the transition from delay to exponential decay.

The resulting fit parameters include the background concentration C_{BG} and the decay parameter τ, while the start concentration used for the fits, $C(t_{start} + \Delta t)$, may differ from the actual start concentration C_{start} within the fluctuations during the equilibrium state.

Since the integral $\int_{t_{start}+\Delta t}^{\infty}(f(t) - C_{BG})dt$ is exactly equal to τ, a good approximation of the AoA of a sensor i is given by $A_i = \Delta t + \tau$. This approximation already completely filters out the interfering influences of background concentrations and finite time series, which is necessary because long-term drifts are common with the type of CO_2 sensor in use.

5 Results

5.1 Comparison of supply-based and distributed CO_2-injection

To compare the AoAs obtained from the different approaches, the averaged AoAs are shown in Fig. 10 in the form of a scatter plot. There, the coordinates represent the AoA values to visualize possible correlations. This is supported by the diagonal line symbolizing equal values for both approaches. Furthermore, the error bars indicate the standard deviation of the values used to calculate the plotted averages of the AoAs for the room's exhaust and the breathing zone for all the ventilation scenarios documented in Tab. 1.

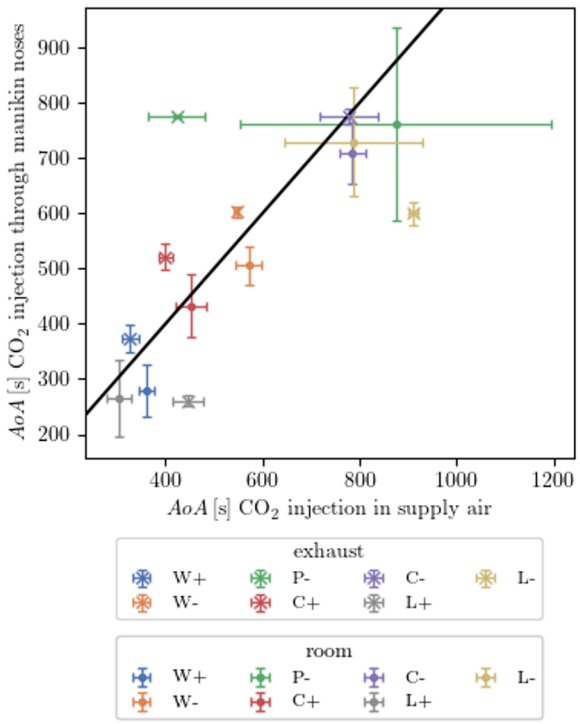

Fig. 10. Comparison of the mean AoAs based on the CO2 injection into the supply air and the exhalation simulation. Tuples for all scenarios as well as for the exhaust and the room's breathing zone are illustrated. Error bars represent the standard deviation of the mean values.

Overall, the results show that there is a good correlation between the AoAs of the different approaches in the different scenarios. This is especially true for the cases of mixing ventilation, i.e for the wall and ceiling unit scenarios.

Significant deviations from the overall correlation are shown for the exhaust values of the parapet unit and the low-momentum ventilation concept. The latter exhibits significantly lower AoA values for the exhaust estimated with distributed injection than for the supply air injection. This is due to the fact that without predominant mixing, a significant part of the room is already filled with fresh air when the distributed injection is switched off. The more complex question is why this effect is not so pronounced with the sensors in the breathing zone of the room. For that, an uneven spatial distribution of the AoAs could be the reason.

For the parapet unit, the low exhaust AoA for the injection into the supply air is an indication that a significant part of the flow is short-circuited between the inlet and the outlet. This effect is only found for the time of supply air injection, because with distributed injection the fresh air short circuit is already present during the equilibrium phase before decay and is therefore no longer present with regard to the exponential decay period.

Furthermore, even for the mixing ventilation cases W and C, the AoA based on the breathing simulation tends to overestimate the exhaust value and underestimate the value for the breathing zone of the room. Based on the overestimation of the exhaust value, we attribute this to the fact that small fractions of the flow are short-circuited.

In terms of the derived performance of the different concepts, smaller AoA values are preferable. This means that of the units providing a mixing ventilation, the wall-mounted unit performs better than the ceiling-mounted unit for both flow rates. In particular, for the low flow rate operation, it still provides AoAs of 500 s to 600 s, while the corresponding values of all the other concepts are about 800 s and show large deviations related to the spatial positions of the sensors.

The performance of the low-momentum ventilation is also noteworthy. It achieves AoA values of about 300 s for the breathing zone, which represents the fastest air exchange of all concepts tested. Yet, unlike a similarly performing wall-mounted unit, it is more dependent on a higher flow rate, as the values for the L- case also lie within the cluster around an AoA of 800 s.

5.2 Comparison of CO_2 and aerosol decay

Fig. 11 shows the averaged AoAs determined by the concentration decay obtained during the aerosol distribution test series in relation to the values obtained by the standard method of injection into the supply air. The figure is composed in the same way as Fig. 10 by incorporating the data from the aerosol tests of both source positions. The aerosol AoA is thus based on the decay data of number-based concentration for the size fraction 0.3 to 2.5 µm.

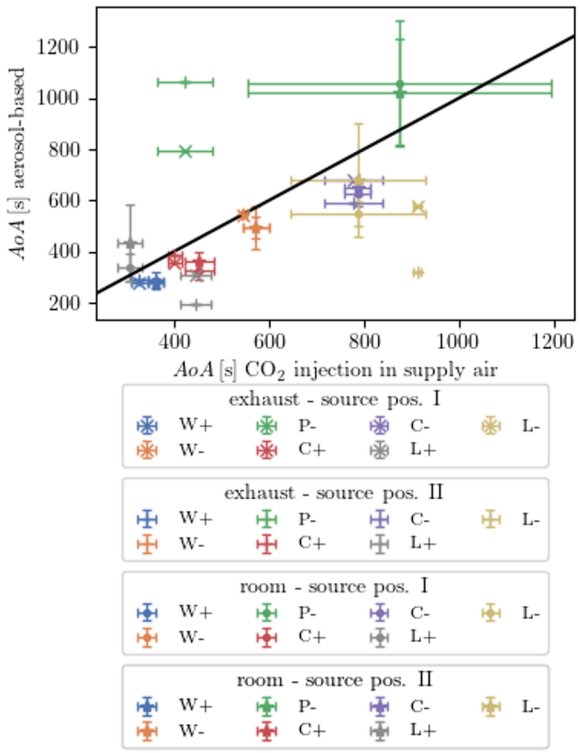

Fig. 11. Comparison of the mean AoAs based on the CO2 injection into the supply air and the aerosol trials. Tupels for all scenarios, the exhaust and the room's breathing zone and the two aerosol source positions are illustrated. Error bars represent the standard deviation of the mean values.

This plot largely reflects the same features as Fig. 10, namely the overall correlation between the compared approaches and the concept-specific deviations for the parapet unit and the low-momentum concepts. In addition, it is found, that the aerosol-based AoAs predominantly underestimate the values determined by CO_2 injection into the supply air. We attribute this result to the fact, that the particle concentration undergoes an additional, non-negligible decrease in concentration due to deposition on surfaces.

5.3 Resulting temperatures

With the objective to assess the effectiveness of the heat recovery system, the mean temperature differences ΔT between the sensors on the desks and the environmental temperature of about 10-11 °C are shown in Fig. 12.

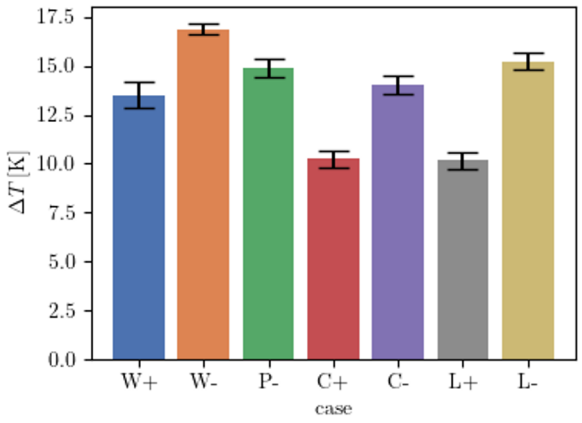

Fig. 12. Temperature differences ΔT between the mean temperature near the thermal manikins and the environmental temperature for the different cases. The error bars indicate the temporal-spatial standard deviation.

The plot depicts that the temperature differences range from 10 K to 17 K. The main relation is that higher flow rates results in lower room temperatures and vice versa. Further, the ventilation of the wall-mounted unit yields 2…3 K higher indoor temperatures than the other concepts for the respective flow rates. Yet, further investigations are necessary to determine whether this difference is caused by the characteristics of the large-scale flow pattern or depends on the efficiency of the ventilation unit. With respect to the set environmental temperatures, the displayed differences can be associated with the subjective assessments from slightly cold to too hot. This means, that for the given environmental temperature, a comfortable setting can be found by adjusting the flow rate of the units and without an additional heating demand.

6 Conclusion

In the present paper we introduced a test environment representing a generic conference room, which allows to investigate different ventilation solutions at full scale with realistic obstructions and thermal boundary conditions.

We investigated three different mixing ventilation concepts based on different ventilation units and a low-momentum ventilation concept.

These concepts were analyzed in terms of general air exchange (tracer gas injection into supply air), exhalation simulation, and aerosol distribution, while additionally recording the temperature.

The results reveal that the AoA values of all approaches can be used to estimate the performance of different ventilation concepts, especially when they are based on mixing ventilation. However, the AoA results of the different approaches are quantitatively different, which means that the results of different approaches should not be used to compare different solutions. Also, less conventional concepts, such as the parapet unit, showed large deviations between the results of the different approaches, highlighting that such concepts always need a higher investigation effort to be fully characterized.

The main purpose of this first evaluation is to compare the different measurement methods. With the available data and the spatial distributions contained therein, the advantages and disadvantages of the individual ventilation concepts in terms of air quality and temperature, will be examined in more detail in further studies.

Acknowledgement

This work was supported by the German Federal Ministry for Economic Affairs and Climate Action (ZIM grant number KK5300001TS1). The authors would like to thank MultiCross GmbH for providing the ventilation units and Robert Brinkema for his work on the project.

References

1. Y. Zhang, G. Feng, Z. Kang, Y. Bi, Y. Cai: "Numerical Simulation of Coughed Droplets in Conference Room", Procedia Eng., **205**, pp. 302-308 (2017). doi: 10.1016/j.proeng.2017.09.981
2. M. Abuhegazy, K. Talaat, O. Anderoglu, S.V. Poroseva: "Numerical investigation of aerosol transport in a classroom with relevance to COVID-19", Phys. Fluids, **32**, 103311 (2020). doi: 10.1063/5.0029118
3. S. Merbold, G. Hasanuzzaman, T. Buchwald, C. Schunk, D. Schmeling, A. Volkmann, R. Brinkema, U. Hampel, A. Schröder, C. Egbers: "Reference experiment on aerosol particle transport for dynamic situations", Tech. Mess., **90**, pp. 340-352 (2023). doi: 10.1515/teme-2022-0118
4. C.-A. Roulet, P. Cretton: "Field Comparison of Age of Air Measurement Techniques", Roomvent'92, pp. 213-229, (1992).
5. P. Lange, D. Schmeling, A. Westhoff. J. Bosbach: "Cost-effective human comfort manikin with realistic thermal load for studies of convection-driven ventilation systems", PROCEEDINGS — Roomvent & Ventilation 2018, pp. 367-372 (2018).
6. K. Azuma, N. Kagi, U. Yanagi, H. Osawa: "Effects of low-level inhalation exposure to carbon dioxide in indoor environments: A short review on human health and psychomotor performance", Environ. Int., **128**, pp. 51-56 (2018). doi: 10.1016/j.envint.2018.08.059
7. M.M. Andamon, P. Rajagopalan, J. Woo: "Evaluation of ventilation in Australian school classrooms using long-term indoor CO2 concentration measurements", Build. Environ., **237**, 110313 (2023). doi: 10.1016/j.buildenv.2023.110313
8. D. Schiepel, R. Brinkema, D. Schmeling: "Artificial saliva aerosol source and detection system for spreading analysis in indoor environments", INDOOR AIR 2022, (2022).
9. K. Niehaus, A. Westhoff: "An open-source data acquisition system for laboratory and industrial scale applications", Meas. Sci. Technol., **34**, 027001 (2023). doi: 10.1088/1361-6501/ac9994
10. American Society of Heating, Refrigerating and Air-Conditioning Engineers, Inc., ANSI/ASHRAE Standard 129-1997 (RA 2002) "Measuring Air-Change Effectiveness" (2002).